THE JOURNAL OF PHYSICAL CHEMISTRY A

Article

pubs.acs.org/JPCA

# Matrix Isolation Study of the Conformations and Photochemistry of S-Ethyl Fluorothioformate, $FC(O)SCH_2CH_3$

Lucas S. Rodríguez Pirani,[†] Mauricio F. Erben,*[,†] Helge Willner,[‡] Rosana M. Romano,[†] and Carlos O. Della Védova*[,†]

[†]CEQUINOR (CONICET-UNLP), Departamento de Química, Facultad de Ciencias Exactas, Universidad Nacional de La Plata, C. C. 962 (1900) La Plata, República Argentina

[‡]Fachbereich C-Anorganische Chemie, Bergische Universität Wuppertal, Gaußstrasse 20, 47097 Wuppertal, Germany

Supporting Information

**ABSTRACT:** The IR spectra of S-ethyl fluorothioformate, $FC(O)SCH_2CH_3$, were recorded in the vapor phase and compared with the Raman spectrum in the liquid state. Additional IR spectra of the compound isolated in argon and nitrogen matrices at ca. 12 K were also recorded. The title compound exhibits rich conformational equilibria at room temperature being $C_1$ the most stable symmetry with a synperiplanar orientation of the carbonyl double bond (C═O) with respect to the S−C($sp^3$) single bond, while the C−C bond of the ethyl group presents a gauche orientation with respect to the C−S single bond. Several bands assigned to a second conformer were also observed in the IR matrix spectra. This second rotamer presents a planar skeleton ($C_s$ point group) retaining the prevalent syn orientation of the $FC(O)SCH_2CH_3$ molecule with an antiperiplanar orientation of the C−C bond of the ethyl group with respect to the C−S bond. The variation of the nozzle temperature before matrix gas deposition gives rise to different conformer ratios. With these data an enthalpy difference of 0.45 kcal $mol^{-1}$ can be calculated between the more stable $C_1$ and the $C_s$ conformers. A third form, corresponding to the anti-gauche conformer, is also detected when the matrix is exposed to broad-band UV−visible irradiation. Moreover, the photochemistry of the Ar and $N_2$ matrix-isolated species is studied. Conformational interconversion is observed at short irradiation times, whereas a decarbonylation process with the concomitant formation of a $HC(S)CH_3$:HF molecular complex dominates the photochemistry of $FC(O)SCH_2CH_3$ of longer irradiation times. The new ethyl fluoro sulfide, $FSCH_2CH_3$, is proposed as an intermediate species.

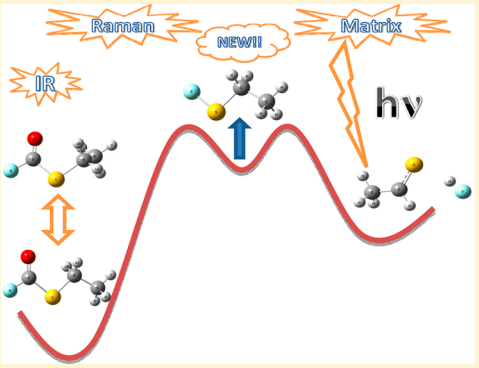


## 1. INTRODUCTION

The geometry and conformation of sulfenylcarbonyl compounds of general formula XC(O)SY have been largely studied by using different spectroscopic techniques, which include gas electron diffraction,[1−6] microwave spectroscopy,[7−9] low-temperature X-ray diffraction,[10−13] and vibrational spectroscopies,[14−16] among others. The relation with biomolecules possessing the −SC(O)− moiety, such as the coenzyme A,[17−19] is one of the reasons that inspired our investigations. In this context, the conformational properties around the central −SC(O)− group become relevant, and efforts to elucidate their behavior were performed. There exists abundant experimental evidence about the essentially planar structure of the XC(O)SY skeleton, which gives rise to syn [$\tau$(O═CSY) = 0°] and anti [$\tau$(O═CSY) = 180°] conformational options (see Figure 1),[20] the former being strongly preferred. These conformational preferences have been rationalized mainly on the basis of the anomeric effect.[11,21]

The analysis of simple members of this family, such as those molecules with X being a halogen atom, revealed some interesting trend. For ClC(O)SY (Y = Cl, NCS, $CH_3$, $CH_2CH_3$) species,[16,22,23] the syn conformation has been observed in the gas phase at room temperature in most cases without evidence of a second rotamer in equilibrium. However, when X = F the abundance of the anti conformer in the same conditions increases.[3] Early gas electron diffraction studies of ClC(O)SCl showed that only the syn form is present,[1] while for FC(O)SCl a composition of roughly 90:10 was determined

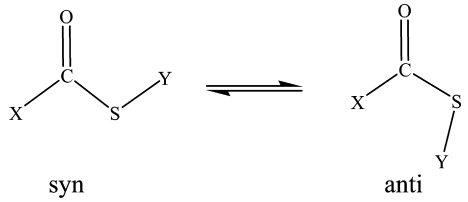


**Figure 1.** Conformational equilibrium around the C−S bond of XC(O)SY molecules.

**Received:** August 4, 2014
**Revised:** October 14, 2014
**Published:** November 3, 2014

   dx.doi.org/10.1021/jp507863b | J. Phys. Chem. A 2014, 118, 11193−11203

at room temperature. A similar result emerges when ClC(O)-$SCF_3$ and FC(O)$SCF_3$ are compared.[3]

The rotameric composition in conformational equilibrium is usually affected by broad-band UV−visible irradiation of matrix isolated species, probably through a mechanism that involves the population of particular excited states. In a recent matrix isolation study on methyl thiofluoroformate, FC(O)$SCH_3$, photoisomerization of the syn into the anti form occurred, followed by the elimination of CO with the concomitant formation of the novel and simple $CH_3SF$ sulfide.[24]

The reported study of FC(O)$SCH_3$ opened an intriguing question. In terms of its conformational equilibrium this molecule differs from its XC(O)SY congeners. Thus, in spite of the inherent electronegativity of the fluorine attached to the sulfenylcarbonyl moiety the abundance of its second anti conformer differs from the expected ca. 10% abundance in agreement with the general picture. Therefore, and to validate the importance of the properties of the $CH_3$ group in the augmented stability of syn FC(O)$SCH_3$, we would like to put into consideration its analogue FC(O)$SCH_2CH_3$.

The first investigations related to the conformational properties of ethyl thioesters, of the general formula XC(O)-$SCH_2CH_3$ (X = H, Cl, F, CN, $CF_3$) were performed nearly 30 years ago by True and Bohn using low resolution microwave spectroscopy.[8,9] In all cases, the syn structure was determined to be more stable than the anti planar structure around the XC(O)S− skeleton. Moreover, ethyl derivatives could also adopt different conformations depending on the orientation of the $-CH_2CH_3$, represented by different C−S−C−C dihedral angle values.

The title molecule was first synthesized in 1965 by Olah[25,26] and was studied as precursor for carbocations in superacidic conditions.[27] For FC(O)$SCH_2CH_3$, the low-resolution microwave spectra were interpreted in terms of a mixture of conformers that present a syn conformation of the O═C−S−C dihedral angle connected with gauche or anti orientations about the C−S−C−C dihedral angle.[8] To the best of our knowledge, no other studies are available for this species. The IR matrix isolation spectroscopy has shown to be a very well-suited technique for the study of conformational equilibrium in related species, such as ClC(O)$YCH_2CH_3$ (Y = O[27] and S[23]). Thus, in this work, the conformational equilibrium of FC(O)$SCH_2CH_3$ is studied by using Fourier transform infrared (FTIR) matrix isolation techniques. Thermodynamic parameters are obtained by using different temperatures of the deposition nozzle. The photoevolution channels after broad-band UV−visible irradiation using solid Ar and $N_2$ matrix are also evaluated.

## 2. EXPERIMENTAL SECTION

**2.1. Synthesis and Characterization.** S-ethyl chlorothioformate was synthesized using triphosgene and ethanethiol in the presence of triethylamine, according to the following equation:[28]

$$Cl_3COC(O)OCCl_3 + 2CH_3CH_2SH \rightarrow Cl_3COC(O)SCH_2CH_3 + ClC(O)SCH_2CH_3 + 2HCl$$

The liquid products were fractionally distilled and subsequently purified several times by fractional condensation at reduced pressure to eliminate volatile impurities. S-ethyl chlorothioformate was carefully checked by IR (vapor) and Raman (liquid) spectroscopy.[23]

FC(O)$SCH_2CH_3$ was obtained by reacting S-ethyl thiochloroformate, ClC(O)$SCH_2CH_3$, with thallium fluorine, TlF, according to the following reaction:

$$ClC(O)SCH_2CH_3 + TlF \rightarrow FC(O)SCH_2CH_3 + TlCl$$

Conventional vacuum techniques were used to condense S-ethyl chlorothioformate on TlF into a 90 mL Carius tube equipped with a glass valve and poly(tetrafluoroethylene) stem. Then, the reaction mixture was heated to 70 °C for 7 h. Subsequently, the reaction products were separated in vacuum through traps held at −30, −60, and −196 °C. FC(O)-$SCH_2CH_3$ is a pale yellow liquid and was retained in the −60 °C trap. The reaction yield was nearly quantitative. The title molecule was exhaustively characterized by FTIR, UV−vis, and NMR spectroscopies and vapor pressure measurements (see Supporting Information, Figures S1−S6). Two NMR signals appear in the $^1$H NMR spectrum at 3.36 (2H, qd, $^3J_{H,H}$ = 7.4 Hz, $^4J_{H,F}$ = 1.7 Hz, $-CH_2$) and 1.79 (3H, td, $^3J_{H,H}$ = 7.4 Hz, $^5J_{H,F}$ = 1.9 Hz, $-CH_3$) ppm. The $^{19}$F NMR shows a single multiplete signal at 44.8 ppm. The $^1J_{C,H}$ coupling constants were also determined from the $^{13}$C satellites to be 142.9 and 129.0 Hz for the $CH_2$ and $CH_3$ groups, respectively, while the $^1J_{C,F}$ = 361.0 Hz.

**2.2. Matrix-Isolation Spectroscopy.** Two different matrix isolation apparatuses, available at La Plata and at Wuppertal laboratories, were used. Gas mixture of FC(O)$SCH_2CH_3$ with $N_2$ (AGA) in the proportion of ca. 1:1000, prepared by standard manometric methods, was deposited on a CsI window cooled to ca. 10 K by means of a Displex closed-cycle refrigerator (SHI-APD Cryogenics, model DE-202) using the pulse deposition technique in La Plata.[29] The matrix-isolated FTIR spectra were recorded on a Nexus Nicolet instrument equipped with either an MCTB or a DTGS detector (for the ranges of 4000−400 $cm^{-1}$ or 600−180 $cm^{-1}$, respectively). Following deposition and IR analysis of the resulting matrix, the sample was exposed to broad-band UV−visible radiation ($200 \leq \lambda \leq 800$ nm) from a Spectra-Physics Hg−Xe arc lamp operating at 1000 W. The output from the lamp was limited by a water filter to absorb IR radiation and thereby minimize any heating effects. The IR spectra of the matrix with 0.5 and 0.125 $cm^{-1}$ resolution were then recorded at different times of irradiation to monitor closely any change in the spectra.

In a stainless steel vacuum line (1.1 L volume), a small amount of FC(O)$SCH_2CH_3$ (ca. 0.05 mmol) was mixed with a 1:1000 excess of Ar in Wuppertal. For each experiment, ca. 0.6 mmol of this mixture was passed through a stainless steel capillary and a heated quartz nozzle that was placed directly in front of the matrix supported at 14 K. The nozzle temperature was varied between room temperature and 565 K to obtain variable-temperature spectra. Photolysis experiments on the matrixes were undertaken in the UV region by using a high-pressure mercury lamp (TQ 150, Hereaus, Hanau, Germany) in combination with a water-cooled cutoff filter (Schott, Mainz, Germany). IR (matrix) spectra were recorded on a Bruker IFS66v/S FT spectrometer (Bruker, Karlshure, Germany) in the reflectance mode with a transfer optic. A DTGS detector with a KBr/Ge beam splitter in the region of $\tilde{\upsilon}$ = 4000−400 $cm^{-1}$ was used. In this region, 64 scans were coadded for each spectrum by means of apodized resolution of 0.5 $cm^{-1}$.


dx.doi.org/10.1021/jp507863b | J. Phys. Chem. A 2014, 118, 11193−11203

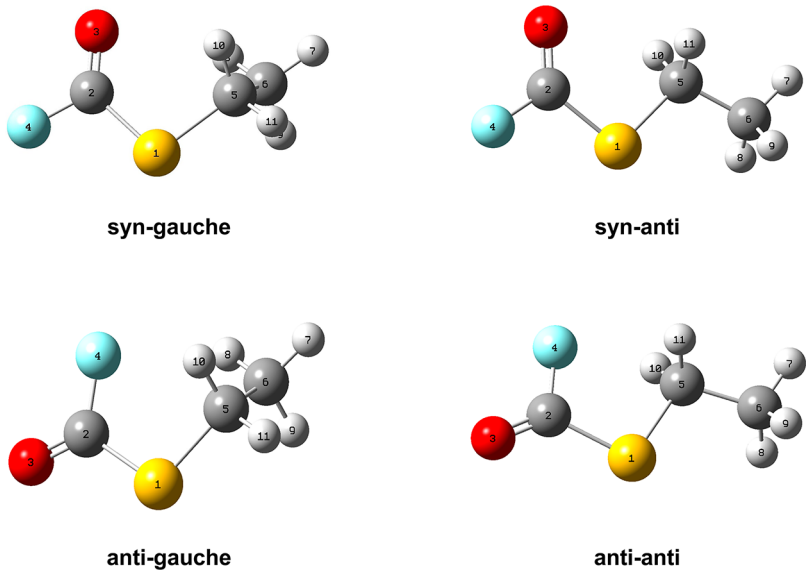


**Figure 2.** Computed stable conformers of $FC(O)SCH_2CH_3$ calculated with the B3LYP/6-311++G** approximation.

**Table 1. Calculated Relative Energies[a] for Stable Conformers of $FC(O)SCH_2CH_3$ in the Ground (in kcal $mol^{-1}$) Electronic States**

| | syn-gauche | | syn-anti | | anti-gauche | | anti-anti | |
|---|---|---|---|---|---|---|---|---|
| | $E°$ | $G°$ | $\Delta E°$ | $\Delta G°$ | $\Delta E°$ | $\Delta G°$ | $\Delta E°$ | $\Delta G°$ |
| B3LYP/6-311++G** | 0.00[b] | 0.00[c] | 0.44 | −0.02 | 2.04 | 2.01 | 2.41 | 2.01 |
| B3LYP/aug-cc-pVTZ | 0.00[d] | 0.00[e] | 0.33 | −0.06 | 2.20 | 2.19 | 2.39 | 2.09 |
| MP2/6-311++G** | 0.00[f] | 0.00[g] | 0.91 | 0.16 | 2.56 | 2.42 | 3.24 | 2.60 |

[a]Including zero-point correction energies. [b]$E^0$ = −690.640 147 hartree (Ha). [c]$G^0$ = −690.671 848 Ha. [d]$E^0$ = −690.676 697 Ha. [e]$G^0$ = −690.708 401 Ha. [f]$E^0$ = −689.421 1227 Ha. [g]$G^0$ = −689.372 234 Ha.

**2.3. Vibrational Spectroscopy.** Gas-phase IR spectra were recorded with a resolution of 1 $cm^{-1}$ in the range of 4000−400 $cm^{-1}$ on the Bruker IFS 66v FTIR instrument, and FT-Raman spectra were run on liquid $FC(O)SCH_2CH_3$ with a Bruker RFS 100/S FT Raman spectrometer. The sample placed in a 4 mm glass capillary was measured using 500 mW of a 1064 nm Nd:YAG laser (ADLAS, DPY 301, Lübeck, Germany).

**2.4. Theoretical Calculation.** Geometry optimization and frequency calculations for different conformers of $FC(O)SCH_2CH_3$ were performed with the GAUSSIAN03 program package[30] (Frisch et al., 2004).[31] MP2 and B3LYP methods employing standard basis sets up to the extended valence triple-$\xi$ basis set augmented with diffuse and polarization functions in both the hydrogen and heavy atoms (6-311++G** and aug-cc-pVTZ) are used.

## 3. RESULTS AND DISCUSSIONS

**3.1. Computed Conformational Properties and Structure.** According to previous studies,[8,9] four conformers could be expected for the title species depending on the relative orientation around the $C(sp^2)$=O and S−$C(sp^3)$, and around the $C(sp^2)$−S and C−C bonds (see Figure 2). Two of these forms were observed in the low-resolution microwave spectrum, with B + C values of 3017(3) and 3597(1) MHz assigned to the syn-anti and syn-gauche conformers, respectively.[8] We analyzed the conformation space by using quantum chemical calculations, and our results reproduce very well this picture. The potential energy curve around CS−C(O) and CC−SC dihedral angles were calculated and are in good accordance with previous reports[23] (see Figure S7, Supporting Information). The syn-gauche conformer is the most stable rotamer in equilibrium with a syn-anti form, which is higher in energy by only 0.33 kcal/mol at the B3LYP/aug-cc-pVTZ level of approximation. The third and fourth conformers, corresponding to the anti-gauche and anti-anti orientations, are calculated at 2.20 and 2.39 kcal/mol above the most stable form (see Table 1).

These energy difference values are in the range of 2 kcal/mol associated with the rule of thumb for relative conformer abundances at room temperature. Thus, we decided to improve the theoretical description available for $FC(O)SCH_2CH_3$ by performing Møller−Plesset calculations at the level of the second order (MP2) to explicitly take into account electron correlation effects. Zero-point corrected electronic energies computed for the four conformers are shown in Table 1. The conformational landscape is equally described by the two methods, the MP2 yielding higher energy differences between the studied conformers.

As far as B3LYP/aug-cc-pVTZ level of approximation is analyzed, the syn-gauche and syn-anti forms (see Figure 2) are the most populated conformer with a abundance of ca. 62.9 and 34.8% at room temperature, respectively. A minor contribution of ca. 1.6 and 0.7% of the anti-gauche and anti-anti conformers, respectively, is expected ($\Delta G°$ = 2.19 and 2.09 kcal/mol). This conformational ratio was obtained from the Boltzmann distribution taking into consideration the computed free energy differences value, $\Delta G^0$, and the degenerations for 2, 1, 2, and 1 for the syn-gauche, syn-anti, anti-gauche, and anti-anti, respectively.


dx.doi.org/10.1021/jp507863b | J. Phys. Chem. A 2014, 118, 11193−11203

**Table 2. Vibrational Spectral Data of S-Ethyl Thiofluoroformate**

| | | matrix | | calculated (B3LYP/aug-cc-pVTZ) | | | | |
|---|---|---|---|---|---|---|---|---|
| IR gas | Raman liquid | Ar | $N_2$ | syn-gauche | syn-anti | anti-gauche | anti-anti | tentative assignment |
| 3599 (<1) | | 3575.3 (<1) | 3577.6 (1) | | | | | 2 $\nu$ (C═O) |
| 3007 (3.1) | | 3004.5 (1.7) | 3004.0 (1.6) | 3128 (2) | 3133 (2) | 3129 (2) | 3137 (2) | $\nu_{as}$ ($CH_2$), $\nu_{as}$ ($CH_3$) |
| | | | | 3110 (1) | 3102 (4) | 3110 (1) | 3102 (3) | $\nu_s$ ($CH_2$), $\nu_{as}$ ($CH_3$) |
| 2987 (5.8) | 2980 (34.8) | 2990.1 (3) | 2988.1 (3) | 3094 (4) | 3098 (2) | 3094 (3) | 3099 (2) | $\nu_{as}$ ($CH_3$) |
| | | | 2985.3 | | | | | |
| 2947 (5.3) | 2941 (100) | 2949 (3) | 2947.0 (4) | 3065 (2) | 3077 | 3063 (1) | 3079 (1) | $\nu_s$ ($CH_2$) |
| | | 2945 | 2938.9 | | | | | |
| 2892 (2.1) | 2882 (24.5) | 2889.2 (<1) | 2888.0 (1) | 3035 (5) | 3038 (4) | 3035 (4) | 3037 (3) | $\nu_s$ ($CH_3$) |
| | | 2882.0 (<1) | 2882.5 | | | | | |
| 1808 (75.7) | 1789 (5.4) | 1802.1 (82) | 1801.0 (83) | | 1840(87) | | | $\nu$ (C═O) |
| | | 1799 | 1798 | | | 1844 (100) | 1844 (100) | |
| | | 1796.9 (73) | 1796.4 (54) | 1838(80) | | | | |
| 1467 (2.1) | | 1468.9 (3) | 1465.4 (3) | 1502 (1) | 1504 (1) | 1502 (1) | 1503 (1) | $\delta_{as}$ $CH_3$ |
| 1459 (2.9) | 1453(8.3) | 1460.9 (4) | 1459.6 (2) | 1492 (2) | 1497 (2) | 1492 (2) | 1496 (2) | $\delta$ ($CH_3$) |
| 1450 (2.4) | 1423 (5.4) | 1452.3 (7) | 1453.9 (6) | | 1482 (1) | | 1484 (1) | $\delta$ ($CH_2$) |
| 1424 (1.8) | | 1421.5 (4) | 1423.1 (4) | 1463 (1) | | 1468 (1) | | |
| 1386 (1.7) | | 1382.2 (4) | 1382.7 (5) | 1418 (1) | 1420 | 1418 (1) | 1419 (1) | $\delta_s$ ($CH_3$) |
| 1297 (1.6) | | 1288.0 (2) | 1290.7 (1.4) | 1307 (3) | 1302 (4) | 1308 (5) | 1301 (6) | wagging $CH_2$ |
| 1273 (3.86) | 1272 (2.5) | 1273.6 (4) | 1276.8 (3) | 1284 (<1) | | 1282 (<1) | | twisting $CH_2$ |
| 1257 (2.2) | | 1257.8 (2) | 1255.2 (1.4) | | 1266 (<1) | | 1268 (<1) | |
| | | | | 1080 (6) | 1079(10) | 1081 (8) | 1083 (10) | rocking $CH_3$ |
| | | 1082 (6) | 1080.1 (10) | 1069 (3) | 1057 (<1) | 1069 (3) | 1052 (<1) | twisting $CH_2$, rocking $CH_3$ |
| 1077 | 1063 (11.2) | 1073.8 (100) | 1070.7 (86) | 1048 (100) | | | | $\nu$ (C−F) |
| 1073 (100) | | | | | | | | |
| 1069 | | | | | | | | |
| 1060 (68.2) | | 1057.0 (92) | 1056.6 (80) | | 1048(100) | | | |
| 1051 (42) | | 1050.0 (59) | 1050.1 (100) | | | | | |
| | | 1028.3 | 1030.0 | | | 1020 (51) | 1030 (60) | |
| | | | 981.6 (2) | | 987 (5) | | 986 (1) | $\nu$ (C−C) |
| 979 | 972 (7.4) | 976 | 975.0 | 977 (4) | | 977 (2) | | |
| 972 (4.5) | | 970 (8) | 970.9 (8) | | | | | |
| 968 | | 967 | 969.3 | | | | | |
| | 769(20) | 767.3(2) | 766.5 (1) | 771 (<1) | 785 (<1) | | 789 (1) | rocking $CH_2$ |
| | | | 760.0 (2) | | | 768 (2) | | |
| 754 | 749 (20) | 750.5 (20) | 749.5 (18) | 748 (6) | 754 (6) | | | $\delta$ (FCO) |
| 750 (2.3) | | | | | | | | |
| 746 | | | | | | | | |
| | | 744.5 | 745.0 | | | 737 (7) | 739 (7) | |
| 667 (1.3) | 664 (47) | 668.0 | 666.7 (4) | 653 (2) | 673 (<1) | 649 (2) | 670 (<1) | $\nu$ (S−$CH_2$) |
| | | 662.2 (11) | | | | | | |
| 646 (4.5) | 644 (8.3) | 644.4 (11) | 644.7 (13) | 643 (1) | 645 (2) | 653 (1) | 644 (2) | $\delta$ ($CO_{o.o.p}$) |
| | 509 (15.7) | 508 | 507 | 500 (<1) | 515 (<1) | 470 (<1) | 493 (1) | $\nu$ (S−CO), $\delta$ (OCS) |
| | 413 (12.7) | 415 | 414 | 409 (<1) | 378 (<1) | 426 (<1) | 394 (<1) | $\delta$ (FCS), $\delta$ (SCC) |
| | 387 (6.8) | | | 312 (<1) | 309 (<1) | 313 (<1) | 303 (<1) | $\delta$ (SCC) |
| | 321 (31.8) | | | 262 (<1) | 243 (<1) | 263 (<1) | 242 (<1) | $\tau$ (HCCH) |
| | | | | 179 (<1) | 145 (<1) | 285 (<1) | 151 (<1) | $\tau$ (HCCS) |
| | | | | 95 (<1) | 114 (<1) | 92 (<1) | 95 (<1) | $\tau$ (FCSC) |
| | 85 (40.6) | | | 79 (<1) | 40 (<1) | 78 (<1) | 53 (<1) | $\tau$ (CCSC) |

For a better description of the structural properties of the most stable syn-gauche conformer, selected structural parameters early reported from the microwave spectrum[8] together with those computed at the B3LYP method are shown in Supporting Information (Table S1).

**3.2. -Vibrational Analysis and Matrix-Isolated Infrared Spectra.** The observed band positions in the IR (gas and matrix) and Raman spectra together with calculated wavenumbers (B3LYP/aug-cc-pVTZ) are collected in Table 2. Figure 3 shows the IR (gas) and Raman (liquid) spectra of $FC(O)SCH_2CH_3$. The 27 normal modes of vibration of each form in equilibrium are all active in both IR and Raman spectra. The assignment of the observed bands is performed by comparison with the calculated spectra, and the approximate description of modes is based on the calculated displacement vectors for the fundamentals as well as on comparison with spectra of related molecules, mainly $ClC(O)SCH_2CH_3$[24] and $FC(O)SCH_3$.[31,32]

The most intense gas-phase IR bands at 1813 and 1073 $cm^{-1}$ can be assigned with confidence to the C═O and C−F


dx.doi.org/10.1021/jp507863b | J. Phys. Chem. A 2014, 118, 11193−11203

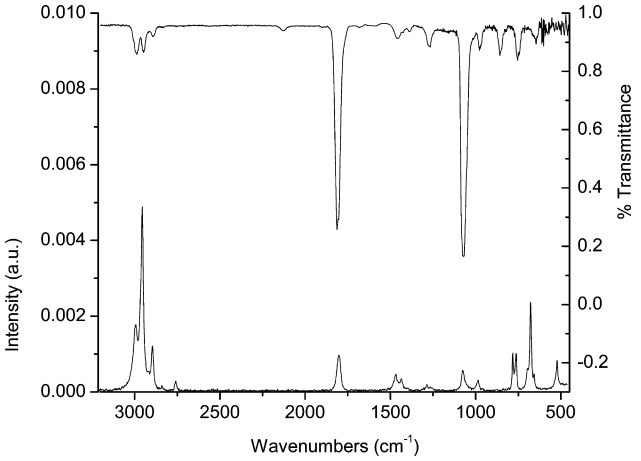


**Figure 3.** Gas IR and liquid Raman spectra of $FC(O)SCH_2CH_3$.

stretching modes, respectively, in agreement with the early assignment reported by Olah and collaborators.[25] Other vibrational modes are clearly observed in the spectrum. The $\nu$(C−C) stretching mode is observed at 972 $cm^{-1}$, whereas the band centered at 750 $cm^{-1}$ is assigned with confidence to the $\delta$(FCO) deformation mode. The C−H stretching region observed between 2987 and 2892 $cm^{-1}$ corresponds to the antisymetric and symmetric stretching bands of the methylene and methyl groups.

The gas-phase IR spectrum seems to indicate the presence of only one conformer. However, the intense band at 1073 $cm^{-1}$, which is assigned to the $\nu$C−F vibrational mode, presents two well-defined shoulders (see Figure 4). These features could

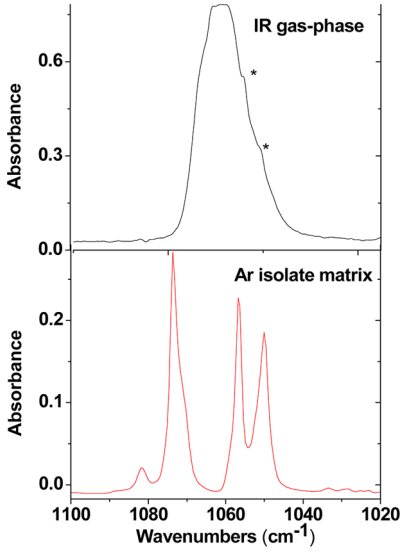


**Figure 4.** Gaseous IR (upper) and Ar isolated matrix IR (lower) spectra of $FC(O)SCH_2CH_3$ in the C−F stretching region. The shoulders marked with asterisks indicate possible contributions of less stable rotamers in the gas-phase spectrum.

indicate the presence of more than one conformer in the gas phase. With the primary aim to elucidate the presence of less stable conformers, the inert gas matrix isolation conditions were used. Figure 4 shows the C−F stretching region of the IR spectrum of $FC(O)SCH_2CH_3$ diluted in Ar matrix (1:1000 ratio), in which three clear signals are observed. These bands at 1073, 1056, and 1050 $cm^{-1}$ are in agreement with the characteristics observed in the IR gas spectrum and could indicate the presence of more than one conformer in the gas phase. Other vibrational regions are taken into account, and a complete analysis is performed in Section 3.3.

On the other hand, in the Raman spectrum of the liquid, the C═O and C−F stretching modes appear at 1789 and 1063 $cm^{-1}$, respectively, as bands with weak intensity (see Figure 3). The most intense signal in the Raman (liquid) spectrum at 2941 $cm^{-1}$ corresponds to the symmetric stretching vibrational mode of the methylene group, whereas the symmetric mode of methyl groups is assigned at 2882 $cm^{-1}$. Other prominent signal in the Raman spectrum at 664 $cm^{-1}$ is attributed to the S−C stretching vibration. This assignment is in agreement with previous results reported for $ClC(O)SCH_2CH_3$[24] and $FC(O)SCH_3$.[24,32]

The $\nu$C═O stretching band centered at 1808 $cm^{-1}$ in the gas IR spectrum is shifted toward higher frequency value, as compared with the $ClC(O)SCH_2CH_3$ (1781 $cm^{-1}$). This is expected from the higher electronegativity of the F atom compared to that of the Cl atom, as early demonstrated by Kagarise for the case of simple carbonyl compounds.[33] The band contour of the C═O stretching mode in the IR (gas) spectrum can be described as B-type with rotational branches PQ−QR separation of 9 $cm^{-1}$ (see Figure S8, Supporting Information). This is in agreement with the presence of syn conformer ($\delta$(OCSC) ≈ 0°), for which the carbonyl oscillator is almost parallel to the B intermediate axis.[34] Following the classical procedure proposed by Seth-Paul,[35] a semiquantitative analysis of the band contours was performed. The syn-gauche conformer belongs to the $C_1$ symmetric point group and can be classified as a prolate asymmetric rotor, with a theoretical asymmetric parameter of $\kappa_{calc}$ = −0.801. Thus, from its rotational constants, the calculated PR separations expected for A-, B-, and C-type bands are 12.2, 9.7, and 18.3 $cm^{-1}$, respectively, in good agreement with the band centered at 1808 $cm^{-1}$ as well as for other structured bands listed in Table 2. However, the rotameric contribution to this bond would correspond to a narrow region between 1838 and 1844 $cm^{-1}$ according the computed results listed in Table 2. Therefore, the contribution of at least the syn-anti form must be taken into account for the evolution of this bond envelopment.

**3.3. -Conformational Equilibrium in Matrix Isolated Conditions.** Table 2 lists also the IR wavenumbers for $FC(O)SCH_2CH_3$ isolated in cryogenic Ar and $N_2$ matrixes. The characteristic narrow absorptions measured in the IR spectra of matrix isolated species, including experiments at different temperature, complemented with conformer interconversion induced upon UV−vis irradiation, allow studying the conformational behavior in great detail.

Figure 5 shows the compared carbonyl stretching region of the IR spectra of $FC(O)SCH_2CH_3$ diluted in Ar and $N_2$ matrix (1:1000 ratio) to detect feasible matrix effects. Two intense absorptions at 1802.1 and 1796.9 $cm^{-1}$ in the Ar matrix spectrum are attributable, in principle, to the C═O stretching vibration of the two conformers. These observations correspond to the two intense absorptions observed at 1801.0 and 1796.4 $cm^{-1}$ in the $N_2$ matrix. The high-frequency absorption is assigned to the syn-anti conformer, whereas the low-frequency absorption is assigned to the syn-gauche conformers, according with theoretical calculation.

It is observed that the relative intensities of the carbonyl absorptions assigned to the syn-gauche and syn-anti conformers are similar when both the Ar and $N_2$ matrixes are compared


dx.doi.org/10.1021/jp507863b | J. Phys. Chem. A 2014, 118, 11193−11203

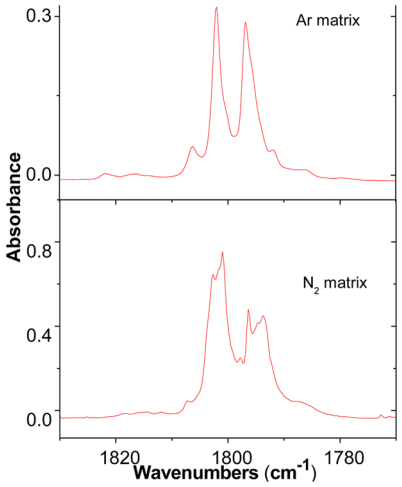


**Figure 5.** FTIR spectra of $FC(O)SCH_2CH_3$ in the region of 1830−1770 $cm^{-1}$ for Ar (upper) and $N_2$ (lower) matrix.

(Figure 5). Small differences can be found for the 1801.0 $cm^{-1}$, whose intensity is slightly higher in the $N_2$ matrix. This fact could be associated with a higher dipole moment for the syn-anti conformer (the computed B3LYP/6-311++G(d,p) values for the syn-gauche and syn-anti conformers are 2.90 and 3.48 D, respectively). In effect, it is usually observed that conformers with high dipole moments are stabilized by the surrounding host, especially in the case of $N_2$ matrix.

Moreover, a third absorption, at intermediate values, is observed in the variable-temperature experiments, as shown in Figure 6. This absorption, located at 1799.0 $cm^{-1}$ in the Ar

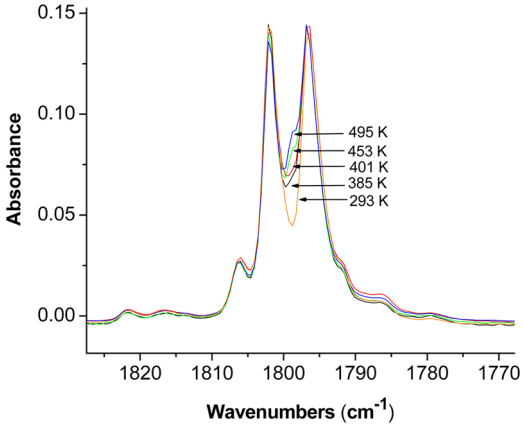


**Figure 6.** IR spectra in the carbonyl stretching region for $FC(O)SCH_2CH_3$ isolated in Ar matrix using different nozzle deposition temperature.

matrix, increases its intensity when the temperature of the deposition nozzle rises. Thus, the presence of a third conformer, likely the anti-gauche, might be expected from these experimental results. Minor absorptions at 1787, 1792, and 1806 $cm^{-1}$ may be originated by the most stable conformer isolated in different cages of the Ar matrix (matrix site effect).

With the aim to obtain the standard enthalpy differences between different conformers, the area ratios of the carbonyl stretching bands belonging to syn-gauche and syn-anti conformers were determined and plotted on a logarithmic scale as a function of the reciprocal absolute temperature. These ratio values correspond closely to the concentration ratios of the two conformers in spite of the similitude of their absorption coefficients. Such a van't Hoff plot based on the $\nu$(C═O) modes (1802/1797 $cm^{-1}$) is shown in Figure 7a. A value of standard enthalpy difference $\Delta H^\circ_{298}$ = 0.45 kcal/mol was derived for this conformational equilibrium in $FC(O)SCH_2CH_3$. Taking into account the calculated (B3LYP/6-311++G**) entropy difference for both conformers ($\Delta S^\circ$ = 1.86 cal/K mol), the standard Gibbs free energy difference ($\Delta G^\circ_{298}$ = −0.095 kcal $mol^{-1}$) is obtained. On the other hand, the van't Hoff plot based on the $\nu$(C−F) modes may be used to calculate the standard enthalpy differences between syn-gauche and anti-gauche conformers. In this region, the band centered at 1028 $cm^{-1}$, which increases its intensity when the temperature of the deposition nozzle rises, was proposed to arise from the anti-gauche forms. Then, the van't Hoff plot for $\nu$(C−F) (1074/1028 $cm^{-1}$) stretching modes belonging to syn-gauche and anti-gauche conformers was also performed (see Figure 7b), and their standard enthalpy difference ($\Delta H^\circ_{298}$ = 2.07 kcal/mol) was obtained. The standard free energy difference ($\Delta G^\circ_{298}$ = 2.12 kcal $mol^{-1}$) was derived of the same form ($\Delta S^\circ$ = 0.167 cal/K mol). It is worth noticing that the excellent agreement between the experimental and computed thermodynamic values describing the conformational equilibrium for the title species.

It is well-known that interconversion between different rotamers isolated in matrix environments can be achieved by irradiating the deposited mixtures with light in the UV−vis range.[36,37] The UV spectrum of gaseous $FC(O)SCH_2CH_3$ presents a very strong absorption below 250 nm, probably associated with the allowed $\pi \rightarrow \pi^*$ transition localized in the FC(O)S− moiety (the spectrum is given as Supporting Information, see Figure S6).

After irradiation with broad-band UV−vis light, some of the IR bands already present in the spectra are observed to grow at the expense of other ones. Figure 8a shows the absorption features of $\nu$(C−F) stretching modes on Ar matrix after irradiation. The absorptions observed between 1080 and 1040 $cm^{-1}$ clearly decrease on irradiation and are assigned to the most stable syn-gauche and syn-anti conformers, while the band centered at 1028 $cm^{-1}$, which grows on photolysis, is proposed to arise from the anti-gauche forms. The 22 $cm^{-1}$ wavenumber difference between these two absorption ($\nu(C-F)_{syn\text{-}anti}$ and $\nu(C-F)_{anti\text{-}gauche}$) forms is in agreement with the results of theoretical calculations, which predict a difference of 28 $cm^{-1}$ (B3LYP/aug-cc-pVTZ), 32 $cm^{-1}$ (B3LYP/6-311++G**), and 36 $cm^{-1}$ (MP2/6-311++G**).

The behavior upon photolysis of the matrix in the FCO deformation spectral region, $\delta$ FCO, is shown in Figure 8b. The band centered at 750 $cm^{-1}$ is assigned to the most stable syn-gauche conformer, while the band at 744 $cm^{-1}$, which grows on photolysis, is proposed to arise from the anti-gauche form. The slight 6 $cm^{-1}$ wavenumber difference between these two absorption is also in agreement with the results of theoretical calculations, which predict a difference of 11 $cm^{-1}$ (B3LYP/aug-cc-pVTZ), 14 $cm^{-1}$ (B3LYP/6-311++G**), and only 2 $cm^{-1}$ (MP2/6-311++G**). These changes were interpreted in terms of an interconversion between different stable conformers of the molecule, involving excited states populated by UV−vis photon absorptions. The features corresponding to the most stable syn-gauche and syn-anti conformers were observed to decrease on photolysis, while the bands of the less stable anti-gauche conformer increase their intensities. Moreover, the assignments for the absorptions belonging to the anti-gauche


dx.doi.org/10.1021/jp507863b | J. Phys. Chem. A 2014, 118, 11193−11203

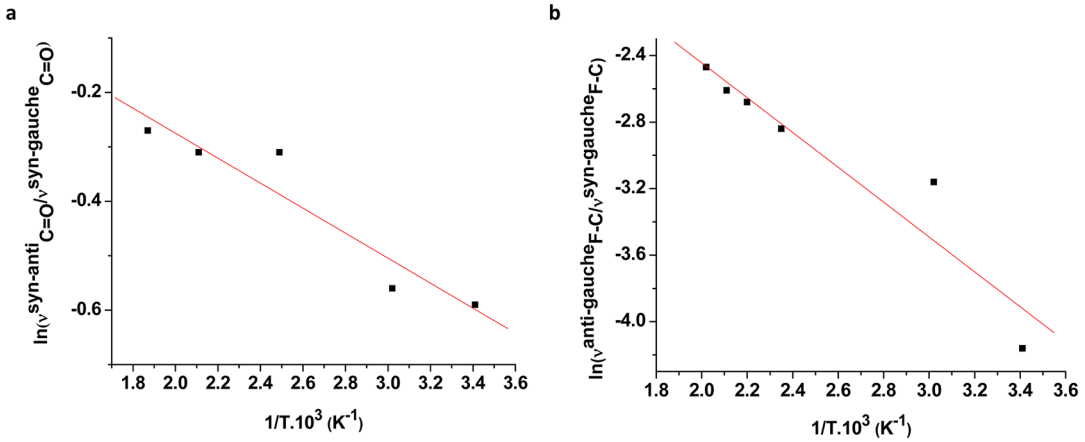


**Figure 7.** van't Hoff plots for the ratios of integrated band areas observed in the IR spectra of $FC(O)SCH_2CH_3$ isolated in Ar matrix isolation experiments at different temperatures of the deposition nozzle. The behavior of the C═O (1802/1797 $cm^{-1}$) and C−F (1074/1028 $cm^{-1}$) stretching modes of $FC(O)SCH_2CH_3$ are shown in the left and right panels, respectively.

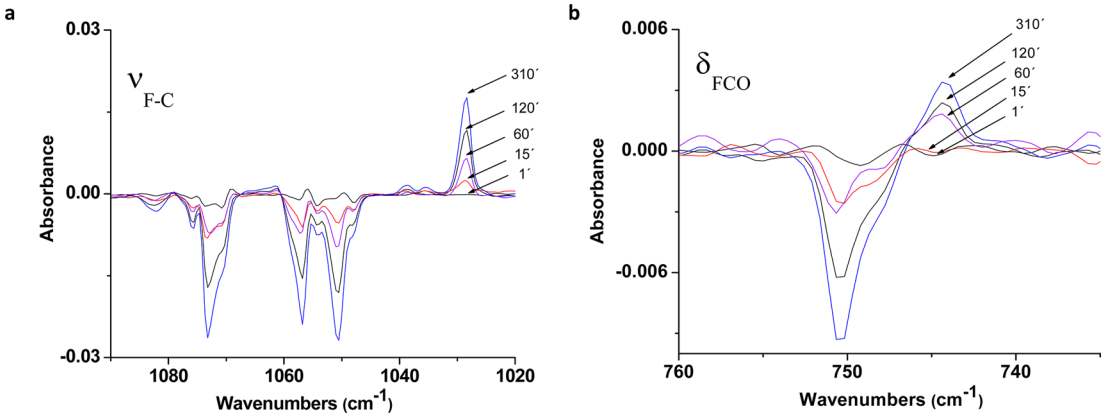


**Figure 8.** Difference IR spectra taken with 0.5 $cm^{-1}$ resolution in Ar matrix containing $FC(O)SCH_2CH_3$ at different times of irradiation after broad-band UV−vis light. (a) 1090−1020 $cm^{-1}$; (b) 760−735 $cm^{-1}$ regions.

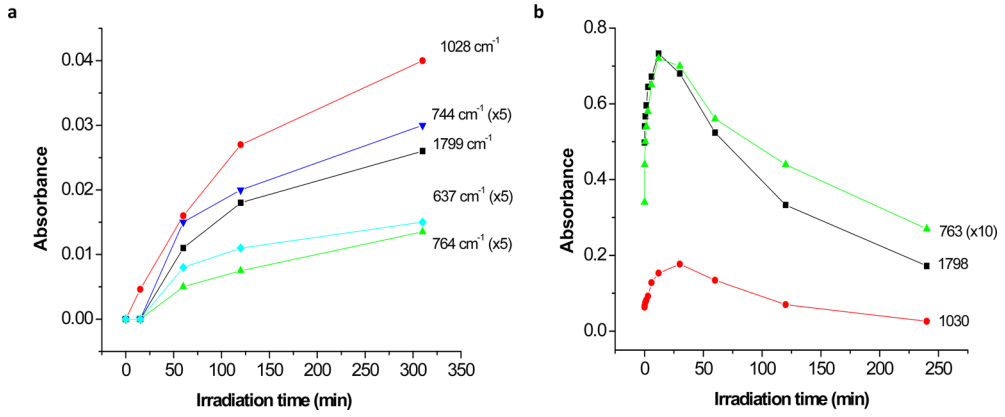


**Figure 9.** Plots as a function of irradiation time of the intensities of the bands assigned to antigauche conformer in Ar (left) and $N_2$ matrix (right).

conformation are further supported by analyzing the behavior of the band intensities as a function of the irradiation time, as shown in Figure 9a.

In agreement with Ar-matrix experiments, the photoisomerization processes are also observed in the IR spectra upon irradiation of the $N_2$ matrix. Photoisomerization occurs in the first step of irradiation and accumulates up to ∼12 min of irradiation when these absorptions decay on continued photolysis, as shown in Figure 9b. At this time, other new bands appear in the spectra.

It is worth noticing that different irradiation lamps are used in the photolysis experiments on Ar and $N_2$ matrixes. When $FC(O)SCH_2CH_3$ in an Ar-matrix is irradiated with a high-pressure mercury lamp the changes in the FTIR spectra can be interpreted as due to the interconversion between different conformers. The same phenomenon is observed when a $N_2$ matrix of the compound is irradiated with a powerful Hg−Xe


dx.doi.org/10.1021/jp507863b | J. Phys. Chem. A 2014, 118, 11193−11203

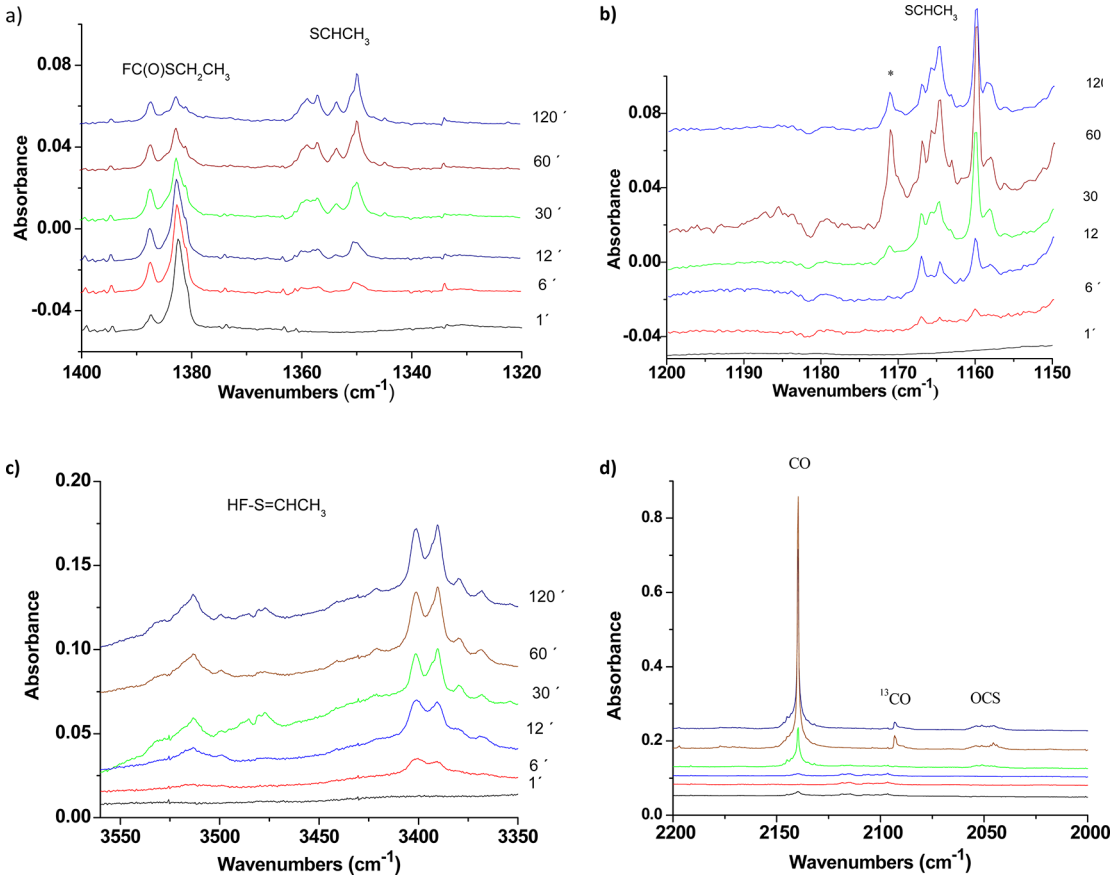


**Figure 10.** FT-IR spectrum for $N_2$ matrix initially containing $FC(O)SCH_2CH_3$ at different irradiation time in the regions (a) 1400−1320 $cm^{-1}$; (b) 1200−1150 $cm^{-1}$; (c) 3560−3360 $cm^{-1}$; (d) 2200−2000 $cm^{-1}$.

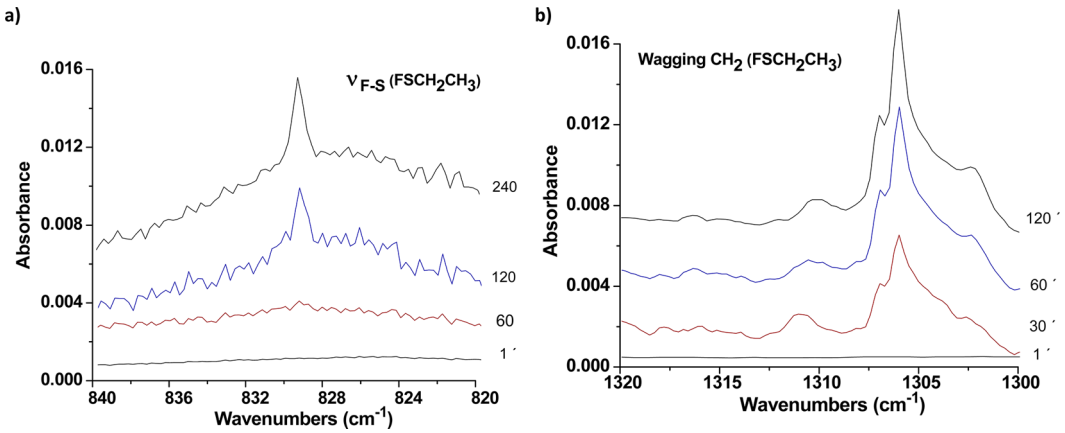


**Figure 11.** FT-IR spectrum for $N_2$ matrix initially containing $FC(O)SCH_2CH_3$ at different irradiation time. The bands observed in the panels (a) and (b) are attributable to the F−S stretching and $CH_2$ wagging normal modes of the $FSCH_2CH_3$ species, respectively.

arc lamp for short periods of times, but photolysis of the sample is observed if the irradiation with the Hg−Xe arc lamp continues for longer times. The photoevolution of the title compound is discussed in the next section.

## 4. PHOTOEVOLUTION OF MATRIX-ISOLATED $FC(O)SCH_2CH_3$

Along with the changes in the IR spectra caused by interconversion of the different rotamers, other bands were observed to appear in the IR spectra upon irradiation of the $N_2$ matrix. In the first step, the production of CO can be clearly observed by the continuous growth of the band at 2138 $cm^{-1}$, characteristic for carbon monoxide isolated in inert matrices (see Figure 10d). The reported frequency value for free CO isolated in a $N_2$ matrix is 2139 $cm^{-1}$, indicating that loosely bound complexes can be present in the matrix cage (see Figure S9, Supporting Information).[38] Such a decarbonylation process should involve the concomitant formation of the $FSCH_2CH_3$ molecule. A similar behavior was reported for the photolysis of the $ClC(O)SCH_2CH_3$ analogue isolated in matrix, for which the formation of CO and $ClSCH_2CH_3$ was proposed as the


dx.doi.org/10.1021/jp507863b | J. Phys. Chem. A 2014, 118, 11193−11203

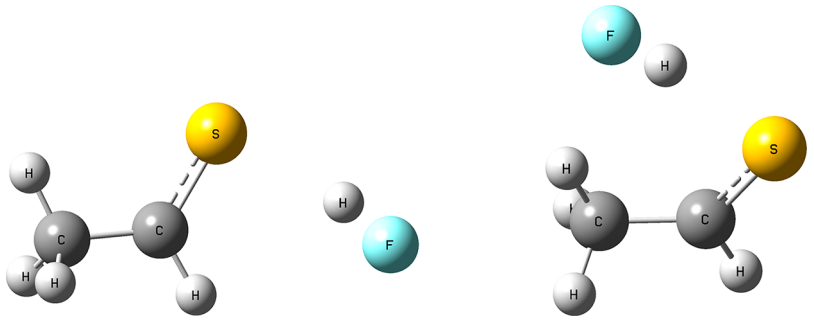


**Figure 12.** Molecular models for two $HC(S)CH_3\cdots HF$ complexes optimized with the B3LYP/6-311++G** theoretical model.

most important decomposition channel after UV−vis irradiation.[23]

To the best of our knowledge, the $FSCH_2CH_3$ sulfide has not been characterized up to now. To identify its presence in our matrix IR spectra, the molecular structure and vibrational frequencies were obtained by using quantum chemical calculation at the B3LYP/6-311++G(d,p) level of approximation. The molecules that belong to the $C_s$ point group of symmetry and the most intense IR absorptions computed for this form are expected to appear at 708 [$a'$, $\nu$(S−F)], 1308 ($a'$ wagging $CH_2$), and 1513 [$a''$, $\delta_{as}(CH_3)$] $cm^{-1}$, the first one being characteristic for this fluorosulfide species (see Figure S10, Supporting Information). The close inspection of the IR spectra gives some evidence of the presence of this species after irradiation of $FC(O)SCH_2CH_3$ isolated in the $N_2$ matrix at cryogenic temperatures. After 120 min of irradiation, the small band centered at 829 $cm^{-1}$ can be observed and may be assigned to the $\nu$(S−F) stretching mode (see Figure 11a). It is plausible that differences between experimental and computed values are due to the formation of loosely bound $FSCH_2CH_3\cdots$CO molecular complexes inside the $N_2$ matrix cage (see Figure S9 in the Supporting Information). Indeed, the proposed assignment is in agreement with the $\nu$(S−F) value of 812 $cm^{-1}$ previously reported for $FSCH_3$, which is formed by the photolysis of $FC(O)SCH_3$ isolated in an Ar matrix.[24] Further evidence for the formation of $FSCH_2CH_3$ comes from the observance of a band appearing at 1306 $cm^{-1}$ after irradiation of the matrix (see Figure 11b), absorption that could be assigned to the deformation normal mode of the $CH_2$ group (wagging), in good agreement with the calculations.

It is important to note, however, the simultaneous appearance of the CO absorption and a signal at very high frequencies, (3513 $cm^{-1}$) characteristic for the HF molecule. Moreover, new features at ∼1358, 1350, 1160, and 745 $cm^{-1}$ also increase their intensities with the irradiation time (Figure 10a,b). These bands can be attributed to the thioacetaldehyde species, $HC(S)CH_3$, in accordance with the reported IR spectrum isolated in Ar matrix, which shows strong absorptions at 1353, 1346, 1141, and 749 $cm^{-1}$.[39,40] The plots as a function of irradiation time of the intensities of the bands assigned to this species are shown in Figure S11 (Supporting Information). It is proposed that thioacetaldehyde is formed through the decomposition of the $FSCH_2CH_3$ intermediate, according to the following reaction scheme:

$$FC(O)SCH_2CH_3 \xrightarrow{-CO} FSCH_2CH_3 \rightarrow HF\cdots HC(S)CH_3$$

It is interesting also to closely analyze the IR features associated with the $\nu$(H−F) stretching mode of the HF molecule, as can be shown in Figure 10c. The HF monomer isolated in an Ar matrix is characterized by $\nu$(HF) = 3953.8 $cm^{-1}$.[41] On the basis of previous studies,[32] the observed red shift of ca. −441 $cm^{-1}$ suggests that a 1:1 hydrogen-bonded complex between HF and $HC(S)CH_3$ is formed. The geometry of two such complexes was optimized by using quantum chemical calculations at the B3LYP/6-311++G** level of approximation. Both species result in minima in the potential energy surface having similar electronic energies. In the equilibrium geometry the H−F axis is directed toward the S atom forming a C═S···HF angle close to 90°, as shown in Figure 12. These models are in accordance with similar complexes between thioformaldehyde and HF or HCl.[22,24] The theoretical values computed for the stretching mode in the HF unit are 3603 $cm^{-1}$ and 3578 $cm^{-1}$ for the complexes shown in the Figure 12 (left and right, respectively), whereas for the free HF it is 3966 $cm^{-1}$, which strengthens the experimental evidence for the proposed mechanism.

Finally, only a minor amount of OCS is formed after photolysis of $FC(O)SCH_2CH_3$, as illustrated in Figure 10d, where a small absorption at ca. 2050 $cm^{-1}$ is observed only at the longest irradiation times. On the other hand, the extrusion of OCS is a dominant channel in the photolysis of the related $ClC(O)SCH_2CH_3$ species.[23]

## ■ CONCLUSION

S-ethyl fluorothioformate, $FC(O)SCH_2CH_3$, has been synthesized and exhaustively characterized by FTIR and Raman spectroscopy. The conformational equilibrium in gas phase was determined. The syn-gauche and syn-anti forms are the most important conformations, and minor contribution of the anti-gauche conformer is observed at room temperature. The formal substitution of a $CH_3$ by a $CH_2CH_3$ group in $FC(O)SCH_2CH_3$ released its conformational properties to a wide number of examples already reported in terms of its rotational equilibrium with a concentration of the anti (the C═O double bond and the S−C single bond in mutual antiperiplanar orientation) conformer much higher than the 10%. Thus, the nature of the alkyl groups seems to play an extraordinary role to stabilize distinctively the most stable syn form in FC(O)SR compounds (R = $CH_3$ and $CH_2CH_3$).

The photoisomerization processes between these stable conformers have been performed using matrix-isolation IR spectroscopy, confirming the proposed assignment to individual conformers. The standard enthalpy differences ($\Delta H^\circ$) characterizing these conformational equilibria have been determined from variable-temperature matrix-isolated experiments. The experimental $\Delta H^\circ$ values for the syn-gauche → syn-anti and syn-gauche → anti-gauche transitions, 0.45 and


dx.doi.org/10.1021/jp507863b | J. Phys. Chem. A 2014, 118, 11193−11203

2.07 kcal/mol, respectively, are in very good agreement with the computed ones.

Concomitantly with the photoisomerization process, irradiation of the isolated species in a $N_2$ matrix with broad-band UV−vis light leads to photoevolution of $FC(O)SCH_2CH_3$. The main channel is related to the extrusion of CO to give $FSCH_2CH_3$ and the subsequent formation of the 1:1 thioacetaldehyde/HF molecular complex.

## ■ ASSOCIATED CONTENT

### Supporting Information

$^1H$ NMR and $^{19}F$ NMR of $FC(O)SCH_2CH_3$ and gas-phase UV−vis spectrum. Gaseous IR spectrum of $FC(O)SCH_2CH_3$ in the C=O stretching region. Calculated geometric parameters and rotational constant (MHz) for the syn-gauche and syn-anti conformers of $FC(O)SCH_2CH_3$. Potential energy curve and vibrational frequencies for $FSCH_2CH_3$ molecule. Plots as a function of irradiation time of the intensities of the bands assigned to syn-gauche and syn-anti conformers in $N_2$ matrix. Molecular model for $FSCH_2CH_3\cdots CO$ complexes optimized with the B3LYP/6-311++G** theoretical model. This material is available free of charge via the Internet at http://pubs.acs.org.

## ■ AUTHOR INFORMATION

### Corresponding Authors

*E-mail: carlosdv@quimica.unlp.edu.ar. (CODV)

*E-mail: erben@quimica.unlp.edu.ar. (MFE)

### Notes

The authors declare no competing financial interest.

## ■ ACKNOWLEDGMENTS

The Argentinean authors thank the Agencia Nacional de Promoción Científica y Técnica (ANPCYT), the Consejo Nacional de Investigaciones Científicas y Técnicas (CONICET), and the Comisión de Investigaciones Científicas de la Provincia de Buenos Aires (CIC), República Argentina, for financial support. They also thank the Facultad de Ciencias Exactas, Universidad Nacional de La Plata, República Argentina, for financial support.

## ■ REFERENCES

(1) Shen, Q.; Hagen, K. Molecular Structure and Conformation of Gaseous Chlorocarbonylsulfenyl Chloride, ClSCOCl, as Determined by Electron Diffraction. *J. Mol. Struct.* **1985**, *128*, 41−48.

(2) Mack, H. G.; Oberhammer, H.; Della Védova, C. O. Conformational Properties and Gas-Phase Structure of (fluorocarbonyl)sulfenyl chloride, FC(O)SCl; Electron Diffraction, Vibrational Analysis, and ab initio Calculations. *J. Phys. Chem.* **1991**, *95*, 4238−4241.

(3) Gobbato, K. I.; Mack, H.-G.; Oberhammer, H.; Ulic, S. E.; Della Védova, C. O.; Willner, H. Structures and Conformations of $CF_3SC(O)F$ and $CF_3SC(O)Cl$: Gas-Phase Electron Diffraction, Vibrational Analysis, and Theoretical Calculations. *J. Phys. Chem. A* **1997**, *101*, 2173−2177.

(4) Erben, M. F.; Boese, R.; Della Védova, C. O.; Oberhammer, H.; Willner, H. Toward an Intimate Understanding of the Structural Properties and Conformational Preference of Oxoesters and Thioesters: Gas and Crystal Structure and Conformational Analysis of Dimethyl Monothiocarbonate, $CH_3OC(O)SCH_3$. *J. Org. Chem.* **2005**, *71*, 616−622.

(5) Shen, Q.; Krisak, R.; Hagen, K. The Molecular Structure of Methyl Chlorothioformate by Gas-Phase Electron Diffraction and Microwave Spectroscopy Data. *J. Mol. Struct.* **1995**, *346*, 13−19.

(6) Della Védova, C. O.; Romano, R. M.; Oberhammer, H. Gas Electron Diffraction Analysis on S-Methyl Thioacetate, $CH_3C(O)SCH_3$. *J. Org. Chem.* **2004**, *69*, 5395−5398.

(7) Fantoni, A. C.; Della Védova, C. O. Microwave Spectrum and Conformational Properties of Methylfluorocarbonyl Disulphide, $FC(O)SSCH_3$. *J. Mol. Spectrosc.* **1992**, *154*, 240−245.

(8) True, N. S.; Clarence, J. S.; Bohn, R. K.; J, S. Low Resolution Microwave Spectroscopy. 12. Conformations and Approximate Barriers to Internal Rotation in Ethyl Thioesters. *J. Phys. Chem.* **1981**, *85*, 1132−1137.

(9) True, N. S.; Bohn, R. K. Low-Resolution Microwave Spectroscopy. III. Three Conformers in Ethyl Trifluoroacetate, Ethyl Chloroformate, and Ethyl Cyanoformate. *J. Am. Chem. Soc.* **1976**, *76*, 1188−1194.

(10) Romano, R. M.; Della Védova, C. O.; Boese, R. Structural Analysis, Matrix Raman Spectra, Syn-Anti Photoisomerization and Pre-Resonance Raman Effect of Fluorocarbonylsulfenyl Chloride, FC(O)SCl. *J. Mol. Struct.* **1999**, *513*, 101−108.

(11) Erben, M. F.; Della Védova, C. O.; Romano, R. M.; Boese, R.; Oberhammer, H.; Willner, H.; Sala, O. Anomeric and Mesomeric Effects in Methoxycarbonylsulfenyl Chloride, CH3OC(O)SCl: An Experimental and Theoretical Study. *Inorg. Chem.* **2002**, *41*, 1064−1071.

(12) Romano, R. M.; Della Védova, C. O. D.; Boese, R.; Hildebrandt, P. Structural and Spectroscopic Characterization of ClC(O)SNSO. A Theoretical and Experimental Study. *Phys. Chem. Chem. Phys.* **1999**, *1*, 2551−2557.

(13) Rodríguez Pirani, L. S.; Erben, M. F.; Boese, R.; Pozzi, C. G.; Fantoni, A. C.; Della Védova, C. O. Conformational Preference of Chlorothioformate Species: Molecular Structure of Ethyl Chlorothioformate, $ClC(O)SCH_2CH_3$, in the Solid Phase and NBO Analysis. *Acta Crystallogr., Sect. B* **2011**, *B67*, 350−356.

(14) Della Védova, C. O.; Cutín, E. H.; Varetti, E. L.; Aymonino, P. J. Infrared and Raman Spectra and Force Constants of Chlorocarbonylsulfenyl Chloride, ClC(O)SCl. *Can. J. Spectrosc.* **1984**, *29*, 69−74.

(15) Della Védova, C. O. Spectroscopic Properties of Methyl Thiolfluoroformate, $FC(O)SCH_3$. *J. Raman Spectrosc.* **1989**, *20*, 483−488.

(16) Romano, R. M.; Della Védova, C. O.; Downs, A. J.; Parsons, S.; Smith, C. Structural and Vibrational Properties of ClC(O)SY Compounds with Y=Cl and $CH_3$. *New J. Chem.* **2003**, *27*, 514−519.

(17) Yang, W.; Drueckhammer, D. G. Understanding the Relative Acyl-Transfer Reactivity of Oxoesters and Thioesters: Computational Analysis of Transition State Delocalization Effects. *J. Am. Chem. Soc.* **2005**, *123*, 11004−11009.

(18) Kang, Y. K.; Han, S. J. Ab Initio Molecular Orbital Calculations on N-beta-Mercaptoethylacetamide and its Derivatives as Model Compounds of Coenzyme A (CoA), Acetyl-CoA, and Malonyl-CoA. *J. Phys. Chem. B* **1997**, *101*, 7001−7006.

(19) El-Assar, A. M. M.; Nash, C. P.; Ingraham, L. L. Infrared and Raman Spectra of S-Methyl Thioacetate: Toward an Understanding of the Biochemical Reactivity of Esters of Coenzyme A. *Biochemistry* **1982**, *21*, 1972−1976.

(20) Hermann, A.; Ulic, S. E.; Della Védova, C. O.; Mack, H. G.; Oberhammer, H. Vibrational Spectra and Structures of Halogencarbonyl Alkyldisulfanes XC(O)SSR with X = F, Cl and R = $CF_3$, CH3. *J. Fluorine Chem.* **2001**, *112*, 297−305.

(21) Gillespie, R. J.; Robinson, E. A.; Pilmé, J. Ligand Close Packing, Molecular Compactness, the Methyl Tilt, Molecular Conformations, and a New Model for the Anomeric Effect. *Chem.—Eur. J.* **2010**, *16*, 3663−3675.

(22) Romano, R. M.; Della Védova, C. O.; Downs, A. J. Matrix Photochemistry of the Chlorocarbonyl Sulfenyl Compounds ClC(O)SY, with Y = Cl or $CH_3$. *J. Phys. Chem. A* **2004**, *108*, 7179−7187.

(23) Ulic, S. E.; Coyanis, E. M.; Romano, R. M.; Della Védova, C. O. S-Ethyl Thiochloroformate, $ClC(O)SCH_2CH_3$: Unusual Conformational Properties? *Spectrochim. Acta* **1998**, *A54*, 695−705.

(24) Romano, R. M.; Della Védova, C. O.; Downs, A. J. Methanesulfenyl Fluoride, $CH_3SF$, a Missing Link in the Family of

Sulfenyl Halides: Formation and Characterization through the Matrix Photochemistry of Methyl Thiofluoroformate, $FC(O)SCH_3$. *Chem.—Eur. J.* **2007**, DOI: 10.1002/chem.200700118.
(25) Olah, G. *Thiolfluoroformates and Method for their Preparation;* Dow Chemical Co: United States, 1965.
(26) Olah, G. A.; Schilling, P.; Bollinger, J. M.; Nishimura, J. Stable Carbocations. CLXIII. Complexing Ionization, and Fragmentative Alkylcarbenium Ion Formation from Alkyl Haloformates, Thiolhaloformates, and Halosulfites with Antimony Pentafluoride. *J. Am. Chem. Soc.* **1974**, *96*, 2221−2228.
(27) Tobón, Y. A.; Di Loreto, H. E.; Della Védova, C. O.; Romano, R. M. Matrix Isolation Study of Ethyl Chloroformate, $ClC(O)OCH_2CH_3$. *J. Mol. Struct.* **2008**, *881*, 139−145.
(28) Salomon, C. J.; Breuer, E. Facile "One-Pot" Preparation of Phosphonothiolformates. Useful Reagents for the Synthesis of Carbamoylphosphonates. *Synlett* **2000**, *6*, 0815−0816.
(29) Perutz, R. N.; Turner, J. J. Pulsed matrix isolation. A comparative study. *J. Chem. Soc., Faraday Trans. 2* **1973**, *69*, 452−461.
(30) Frisch, M. J.; Trucks, G. W.; Schlegel, H. B.; Scuseria, G. E.; Robb, M. A.; Cheeseman, J. R.; Montgomery Jr., J. A.; Vreven, T.; Kudin, K. N.; Burant, J. C.; et al. *Gaussian 03;* Revision B.04; Gaussian, Inc.: Pittsburgh, PA, 2003.
(31) Della Védova, C. O. Spectroscopic Properties of Methyl Thiolfluoroformate, $FC(O)SCH_3$. *J. Raman Spectrosc.* **1989**, *20*, 483.
(32) Romano, R. M.; Della Védova, C. O.; Downs, A. J. Methanesulfenyl Fluoride, $CH_3SF$, A Missing Link in the Family of Sulfenyl Halides: Formation and Characterization Through the Matrix Photochemistry of Methyl Thiofluoroformate, $FC(O)SCH_3$. *Chem.—Eur. J.* **2007**, *13*, 8185.
(33) Kagarise, R. E. Relation between the Electronegativities of Adjacent Substituents and the Stretching Frequency of the Carbonyl Group. *J. Am. Chem. Soc.* **1955**, *77*, 1377−1379.
(34) Erben, M. F.; Della Védova, C. O.; Boese, R.; Willner, H.; Oberhammer, H. Trifluoromethyl Chloroformate, $ClC(O)OCF_3$: Structure, Conformation, and Vibrational Analysis Studied by Experimental and Theoretical Methods. *J. Phys. Chem. A* **2004**, *108*, 699−706.
(35) Seth-Paul, W. A. Classical and Modern Procedures for Calculating PR Separations of Symmetrical and Asymmetrical Top Molecules. *J. Mol. Struct.* **1969**, *3*, 403−417.
(36) Della Védova, C. O.; Mack, H. G. A Matrix Photochemistry Study on (Fluorocarbonyl)Sulfenyl Bromide: The Precursor of Sulfur Bromide Fluoride. *Inorg. Chem.* **1993**, *32*, 948−950.
(37) Fausto, R.; Teixeiras-Dias, J. C. Conformers, Vibrational Spectra and Laser-induce Rotamerization of $CH_2ClCOOH$. *J. Chem. Soc., Faraday Trans.* **1993**, *89*, 3235−3241.
(38) Dubost, H. Infrared Absorption Spectra of Carbon Monoxide in Rare Gas Matrices. *Chem. Phys.* **1976**, *12*, 139−151.
(39) Maier, G.; Flögel, U.; Reisenauer, H. P.; Andes, B. H., Jr; Schaad, L. J. HCl-Abspaltung aus Ethansulfenylchlorid und Chlordimethylsulfid. *Chem. Ber.* **1991**, *124*, 2609−2612.
(40) Suzuki, E.; Watanabe, O.; Happoya, A.; Watari, E. Photolysis of 2-Methylthietane and 2,4-Dimethylthietane in Argon Matrices: Matrix Infrared Spectra of Thioacetaldehyde. *Vibrational Spectrosc.* **1993**, *5*, 353−357.
(41) Andrews, L.; Wang, X. The Infrared Spectrum of $Al_2H_6$ in Solid Hydrogen. *Science* **2003**, *299*, 2049−2052.